Supplementary Information

Evaporative self-assembly of binary mixture of soft colloids

Merin Jose[1], Muraleedharapai Mayarani[1], Madivala G. Basavaraj[2] and Dillip K. Satapathy[1,*]

1. *Soft Materials Laboratory, Department of Physics, IIT Madras, Chennai - 600036, India*
2. *PECS Laboratory, Department of Chemical Engineering, IIT Madras, Chennai, India*

[*] *E-mail: dks@iitm.ac.in*

Microgel particle synthesis and characterization

p-NIPAM microgel particles of two different sizes were synthesised by the following procedure. For the synthesis of the smaller sized particles (diameter d_1), NIPAM and appropriate amount of cross linker, BIS (2.5 mole percent) were dissolved in deionized water and heated in water bath with continuous stirring in nitrogen atmosphere [3]. When the temperature of the reaction mixture equilibrated at 70°C, the initiator potassiumperoxodisulfate (KPS) was added. The reaction bath was maintained at 70°C for about 8 hours and subsequently cooled down to room temperature (25°C). Next, the supernatant was separated by centrifugation and the residue was redispersed in DI water. This cycle was repeated several times. To obtain particles of larger size (diameter d_2), NIPAM, acrylic acid and BIS were dissolved in deionized water and heated in a controlled temperature bath under continuous magnetic stirring and purging of nitrogen gas [2]. Ammonium persulfate (APS) dissolved in DI water (0.078M) is added to the mixture maintained at 45°C to initiate polymerisation. The reaction mixture was heated to 65°C and maintained at this temperature for about 12 hours. Subsequently, the reaction product was cooled to room temperature (25°C). Once again, the microgel particles formed are subjected to several centrifugation and re-dispersion steps. The microgel dispersions were suitably diluted from the mother solution of known concentration and used for the evaporation experiments.

The synthesis of p-NIPAM microgel particles takes place by precipitation polymerisation reaction[4]. The monomer and crosslinker are heated and when the temperature reaches 70°C, the initiator is added which decomposes to generate free radicals. The free radicals attack monomer to form oligomeric radical chains which grows until a critical chain length, and then collapses to form colloidally unstable 'precursor particles' (nuclei). These precursor particles can either deposit onto existing colloidally stable particle or, aggregate with other precursor particles until they form a particle sufficiently large to be colloidally stable. For the synthesis of larger core particles, the initiator was added at a lower temperature (45°C), followed by heating to 65°C at a ramp rate of about 0.5°C/min. The decomposition rate of initiator is decreased at lower temperatures leading to reduced oligomeric radical concentration[2]. This leads to abundance of collapsed nuclei in the reaction mixture which likely favours particle growth mechanisms. When the temperature ramp is completed, majority of the monomers likely get converted to nuclei and precursor particles. The nucleation stage is then followed by nuclei growth to form particles by monomer addition, nuclei absorption, and nuclei aggregation.

Particle sizes were determined using the dynamic light scattering (Nanopartica SZ-100, Horiba Scientific) technique. The autocorrelation function, $g^1(\tau)$, obtained from the DLS measurements is fitted to an exponential decay function, $y = A\ \exp(-x\Gamma) + y_0$.

In colloidal dispersions containing Brownian particles, the autocorrelation is related to the delay time as [1], $g^1(\tau) = A\exp(-Dq^2\tau) + B$, where, $q = \frac{4\pi n}{\lambda}\sin(\frac{\theta}{2})$ is the scattering wave vector, n is the refractive index of the dispersion medium (n = 1.33), $\lambda = 532$ nm is the wave length of the laser, $\theta = 90°$ is the scattering angle and D is the diffusion coefficient. The diffusion coefficient can be estimated from, $D = \Gamma/q^2$, where Γ is obtained from the best fit shown in Fig. S1. Finally, the radius of the particle is determined by using the Stokes - Einstein relation. The DLS measurements were performed at temperatures ranging from 25 to 45°C, at each temperature the sample is allowed to equilibrate for about 15-20 minutes. Diameter at each temperature is estimated by taking mean of five similar measurements. The zeta potential of the two particle types, sample 1 and sample 2 were also measured and found to be -34.5 mV and -30 mV, respectively.

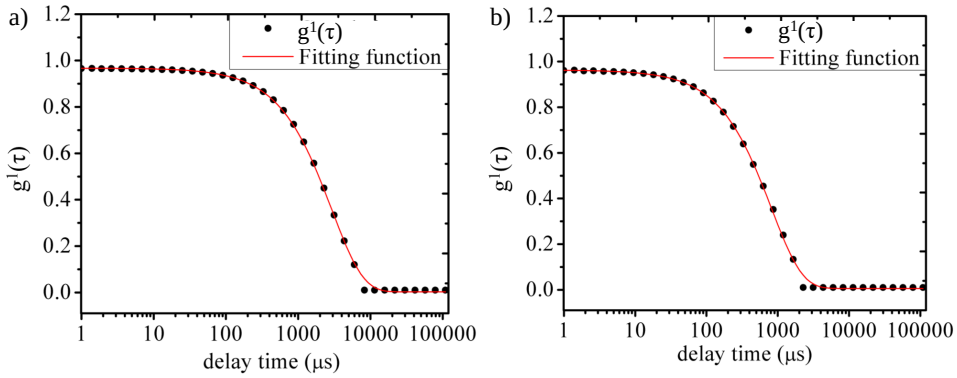

Figure S1: The electric field autocorrelation function Vs. delay time for sample 1 at a) 25°C b) 45°C. Red curves correspond to the exponential fit to the autocorrelation function (see text).

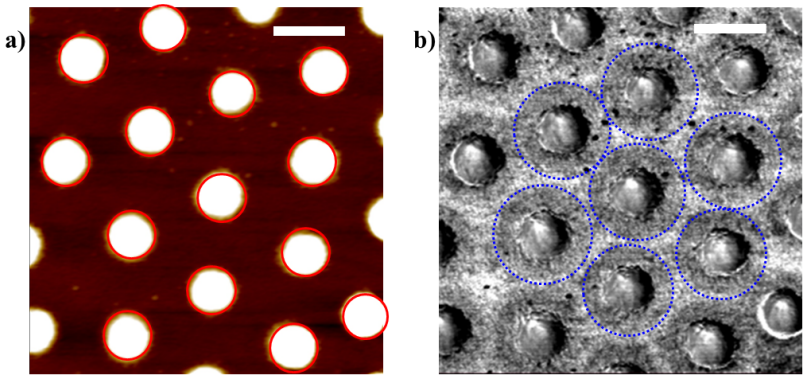

Figure S2: a) AFM image with particle cores encircled in red. b) The corresponding AFM-phase image showing the core+corona architecture of the microgel particles encircled in blue dotted lines. Scale bar : 1μm.

Microstructure of particulate deposits

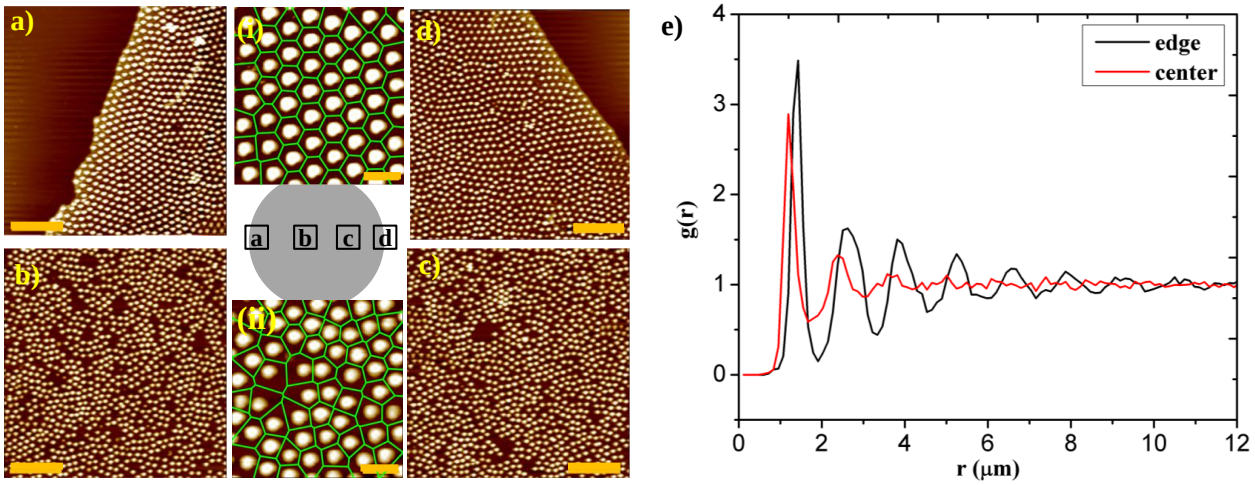

Figure S3: Atomic force microscopy images of different regions of the monolayer deposit formed by the complete evaporation of solvent from a sessile drop containing monodisperse microgel particles having diameter, d_2 = 872 ± 56 nm. The labels (a) to (d) represent different regions of the deposit as indicated in the schematic. Voronoi polygons overlaid on AFM images corresponding to the region near the periphery of the drop showing nearly regular hexagons (i) and corresponding to image near drop center with random polygonal-shaped Voronoi tessellations (ii). Scale bars in images (a - d) corresponds to 10 μm and those in (i and ii) are 2 μm. (e) Pair correlation functions $g(r)$ calculated for a region at the edge (black curve) and near the center (red curve) of the loosely-packed monolayer deposit.

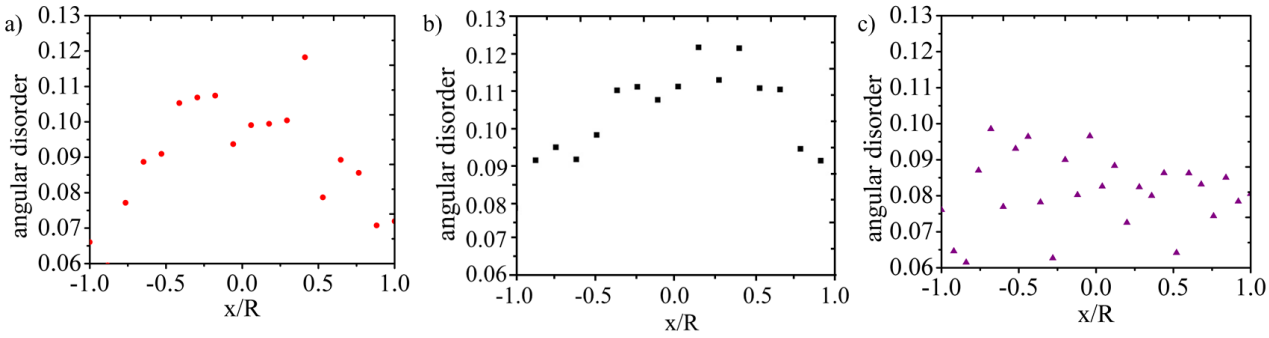

Figure S4: Angular disorder calculated for the monolayer deposit of monodisperse microgel particles (a) of diameter $d_1 = 695 \pm 35$ nm (sample 1) and (b) of diameter $d_2 = 872 \pm 56$ nm (sample 2). The angular disorder that describes the arrangement of microgels in the deposit is estimated by considering the angles of the Voronoi polygons. For ideal hexagonal arrangement of particles all the six angles of the polygon should be 120°. The deviation of the angles from 120° gives the measure of disorder. The data in (a) and (b) show that the angular disorder parameter has a similar trend as the areal disorder with minimum values near the drop edges (x/R = -1, 1) and tending to maximum at the drop center. (c) represents the angular disorder calculated for the monolayer deposit consisting of binary mixture of microgel particles. For the monolayer of bidisperse microgels, the angular disorder does not show any clear the trend like the monodisperse case (see (a) and (b)) and also varies slightly across the deposit. No clear order-to-disorder transition across the deposit is observed for monolayers of bidisperse soft colloids.

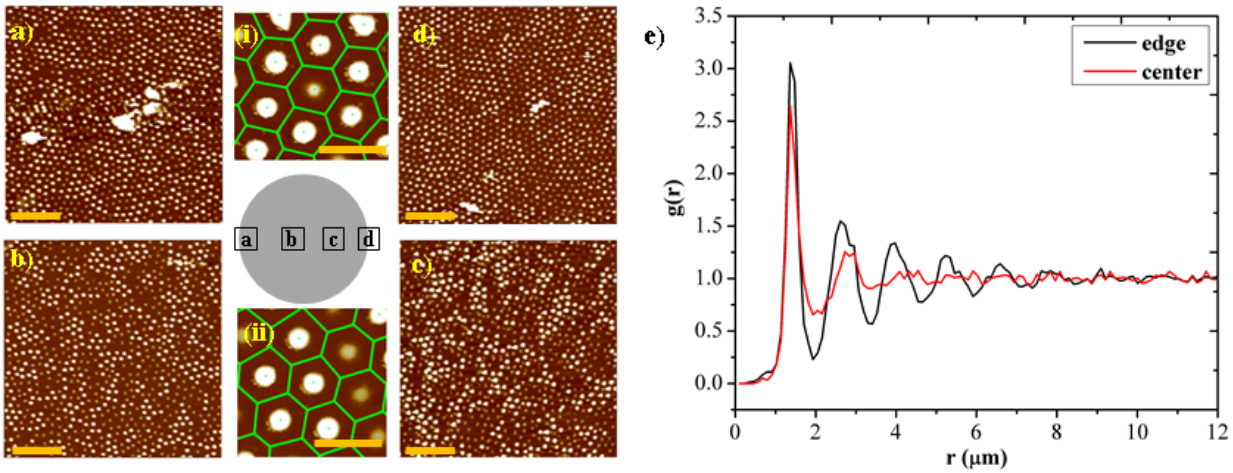

Figure S5: Atomic force microscopy images of different regions of the monolayer deposit formed by the complete evaporation of solvent from a sessile drop containing bidisperse microgel particles with **particle mixing ratio of 1:3 (small:large)**. The labels (a) to (d) represent different regions of the deposit as indicated in the schematic. Voronoi polygons overlaid on AFM images corresponding to a region near periphery of the drop (i) and near drop center (ii) showing nearly regular hexagons. Scale bars in images (a - d) corresponds to 10 μm and those in (i and ii) are 2 μm. (e) Pair correlation functions $g(r)$ calculated for a region at the edge (black curve) and near the center (red curve) of the loosely-packed monolayer deposit. We notice that the pair correlation function for the central region and the edge exhibit a slightly different behaviour (in comparison to mixing ratios, shown in Fig. S6 and Fig. 10 in the manuscript) The differences may arise due to the subtleties during the monolayer transfer at the final drying stages when the liquid line quickly recedes.

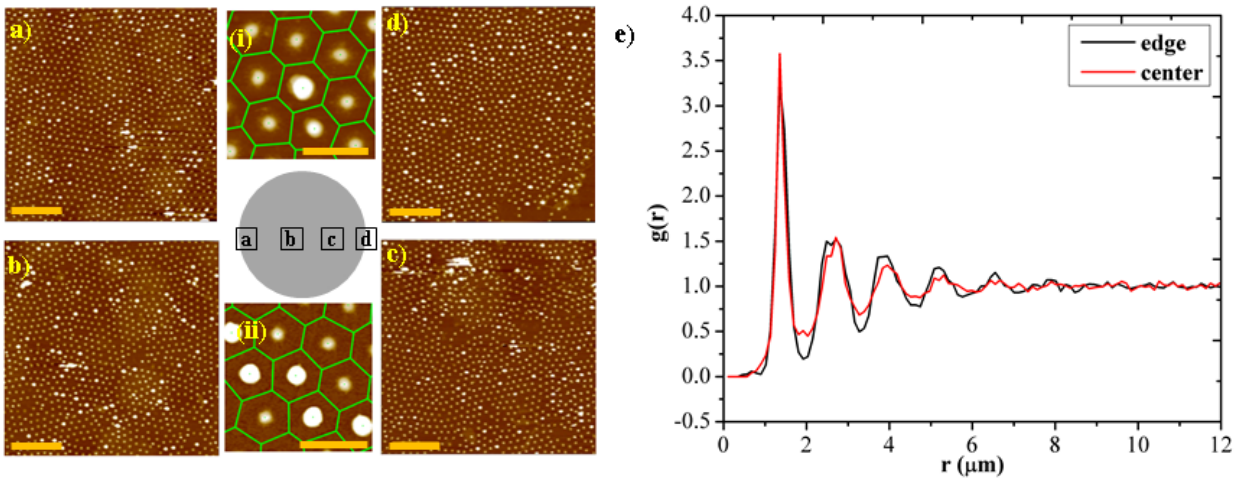

Figure S6: Atomic force microscopy images of different regions of the monolayer deposit formed by the complete evaporation of solvent from a sessile drop containing bidisperse microgel particles with **particle mixing ratio of 3:1 (small:large)**. The labels (a) to (d) represent different regions of the deposit as indicated in the schematic. Voronoi polygons overlaid on AFM images corresponding to a region near periphery of the drop (i) and near drop center (ii) show nearly regular hexagons. Scale bars in images (a - d) corresponds to 10 μm and those in (i and ii) are 2 μm. (e) Pair correlation functions $g(r)$ calculated for a region at the edge (black curve) and near the center (red curve) of the loosely-packed monolayer deposit.

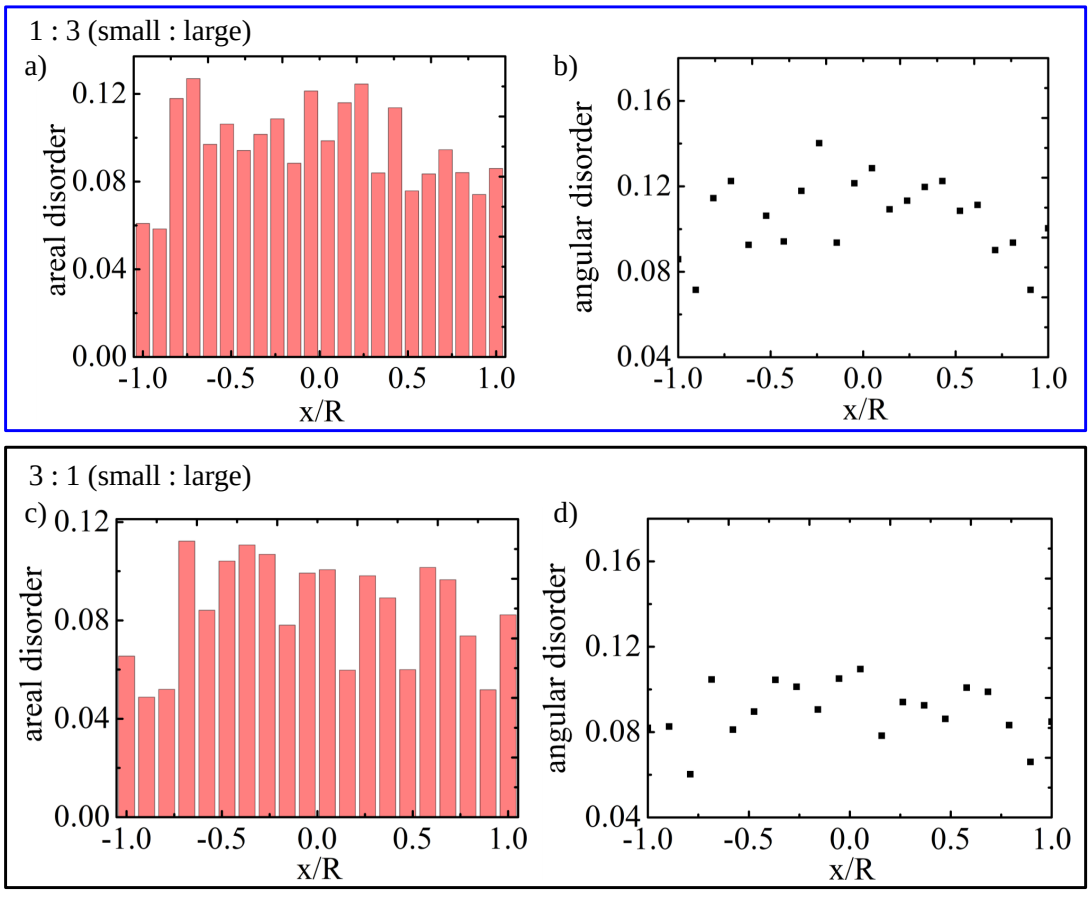

Figure S7: Characterization of distribution of particles across the monolayer deposit formed by the complete evaporation of solvent from a sessile drop containing bidisperse microgels at **1:3 (small:large)** mixing ratio, top panel (inside blue box) and **3:1 (small:large)** mixing ratio, bottom panel (inside black box). a) and c) are areal disorder plots and b) and d) are angular disorder plots.

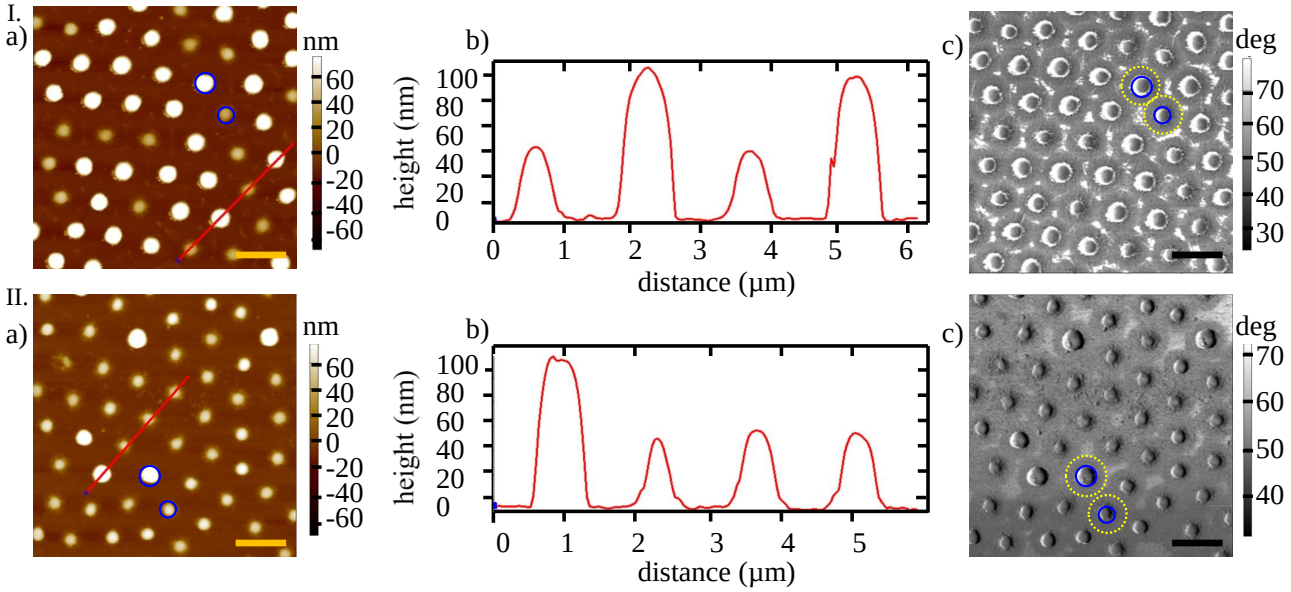

Figure S8: (a) AFM image of the monolayer deposit consisting of binary mixure of microgel particles. The cores of larger and smaller particle are marked with blue circles. (b) Height profile along the red line drawn in the AFM image shown in (a). The height of the smaller particles is nearly three times less than the larger particles. (c) AFM-phase image resolving the core-corona structure of the microgel particles deposited on the solid surface. The particle core is encircled in blue and extent of their coronas is marked in yellow dotted circles. (I, top panel) corresponds to deposits with binary particles at **particle mixing ratio of 1:3 (small:large)** and (II, bottom panel) is for **particle mixing ratio of 3:1 (small:large)**. Scale bars are 2 μm.

Multiple particle tracking microrheology

To study the time evolution of viscoelastic nature of the microgel particle laden water-vapor interface, we have used *multiple-particle tracking microrheology*. First, the video of the entire evaporation process is recorded using an optical microscope fitted with a camera with frame rate of 30 frames per second (fps). While recording, the focus knob of the microscope was continuously adjusted to keep the descending interface at the focal plane of the objective. Next, the relevant frames are extracted from the video at different t/T (t= time and T = total evaporation time) using the ImageJ software. The position coordinates of the tracer PS particles adsorbed at the interface were obtained using a MATLAB routine. The X and Y coordinates of the particles obtained by analyzing a series of frames generates trajectory of the particle adsorbed to the interface. The trajectories of four particles at three different t/Ts (0.2, 0.4 and 0.8) are shown in Fig. S9.

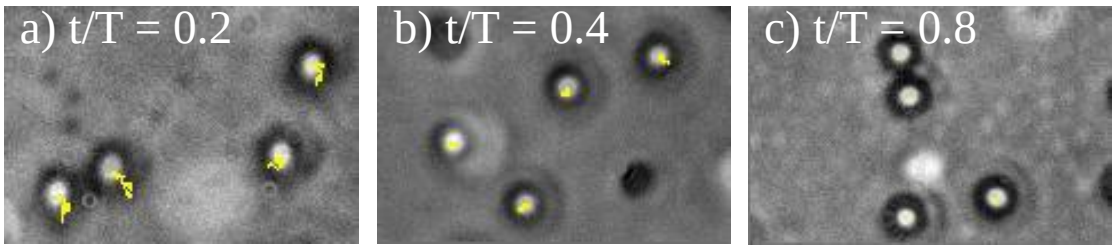

Figure S9: Tracer particles at the p-NIPAM laden interface at a) t/T = 0.2 b) t/T = 0.4 c) t/T = 0.8. The trajectories of the tracers tracked for 1 s are shown in yellow lines. The trajectories get increasingly constrained towards higher t/Ts as the interface becomes almost frozen at t/T = 0.8.

The MSD that is reported is an average of six sets of relative displacements obtained by simultaneously tracking four tracer particles. Most often, the ambient air currents causes a collective drift of the particles adsorbed to the interface. The simultaneous tracking of multiple tracer particles and the calculation of the relative MSDs instead of the absolute MSDs offer a definite advantage in removing the drift induced uncertainties in MSD. The Laplace transform of the measured MSD values ($\langle \Delta \tilde{r}^2(s) \rangle$) is calculated and substituted in the generalized Stokes-Einstein Relation to obtain the frequency-dependent viscoelastic modulus ($\tilde{G}(s)$). The Laplace frequency, $s = 2\pi/\tau$, where τ is the delay time in seconds. Since the delay time is measured from 0.03 second up to 1 second, the frequency ranges from 6 (=$2\pi/1$) to 200 (=$2\pi/0.03$) rad/s. In the Fourier domain (with $s = i\omega$), the $\tilde{G}(s)$ transforms into $G^*(\omega) = G'(\omega) + iG''(\omega)$, whose real and imaginary parts correspond to the elastic and viscous parts of the complex viscoelastic modulus respectively.

References

[1] Puthusserickal A Hassan, Suman Rana, and Gunjan Verma. "Making sense of Brownian motion: colloid characterization by dynamic light scattering". In: *Langmuir* 31.1 (2015), pp. 3–12.

[2] Zhiyong Meng, Michael H Smith, and L Andrew Lyon. "Temperature-programmed synthesis of micron-sized multi-responsive microgels". In: *Colloid and Polymer Science* 287.3 (2009), pp. 277–285.

[3] RH Pelton and P Chibante. "Preparation of aqueous latices with N-isopropylacrylamide". In: *Colloids and Surfaces* 20.3 (1986), pp. 247–256.

[4] Robert Pelton. "Temperature-sensitive aqueous microgels". In: *Advances in colloid and interface science* 85.1 (2000), pp. 1–33.